ELSEVIER

Journal of Hydrology 262 (2002) 209–223

Journal of Hydrology

www.elsevier.com/locate/jhydrol

Development of a snowfall–snowmelt routine for mountainous terrain for the soil water assessment tool (SWAT)

T.A. Fontaine[a,*], T.S. Cruickshank[b], J.G. Arnold[c], R.H. Hotchkiss[d]

[a]*Department of Civil and Environmental Engineering, South Dakota School of Mines and Technology, 501 E. St. Joseph Street, Rapid City, SD 57701 3995, USA*

[b]*Utah State Division of Air Quality, Salt Lake City, UT, USA*

[c]*USDA, Agricultural Research Service, Grassland, Soil and Water Research Laboratory, Temple, TX, USA*

[d]*Albrook Hydraulics Laboratory, Department of Civil and Environmental Engineering, Washington State University, Washington, DC, USA*

Received 12 April 2001; revised 10 January 2002; accepted 14 February 2002

Abstract

The soil water assessment tool (SWAT) is a hydrologic model originally developed to evaluate water resources in large agricultural basins. SWAT was not designed to model heterogeneous mountain basins typical of the western United States, and as a result, has performed poorly when applied to mountainous locations. The intent of this study was to increase the versatility of SWAT by developing the capability to simulate hydrology of a non-agricultural mountainous region with a large snowmelt component. A western Wyoming basin, representative of Rocky Mountain basins, was selected to evaluate model performance, identify governing hydrologic processes, and improve the snowmelt routine. An initial evaluation of SWAT performance indicated an inability of the model to represent snowmelt processes. Based on simulation results and field observations, algorithms were developed which use elevation bands to distribute temperature and precipitation with elevation. Additional routines which control snowpack temperature, meltwater production, and areal snow coverage were designed to simulate the influence of season and elevation on the evolution of basin snowpack. The development of the new snowmelt algorithms improved the average annual Nash–Sutcliffe R^2 correlation between simulated and observed Wind River streamflow from an initial value of -0.70 to $+0.86$.

Keywords: Snowmelt; Hydrology; Modeling; Mountains; Hydrometeorology

1. Introduction

Mountains can be the source of a large fraction of annual streamflow in river basins. Therefore, accurate simulation of hydrologic processes in mountains at large scales is important for water resource management and for local and regional economies. Recent interest in estimating impacts of potential climate change on water resources has also indicated the importance of large-scale simulation of mountain hydrology.

Large-scale hydrologic modeling in mountainous terrain is difficult because extreme elevation gradients, inaccessibility, and low population densities contribute to poor data resolution (Davis and Marks, 1980; Marks et al., 1992). Two of the more dominant mountain hydrologic processes, snowfall and snowmelt, also complicate the simulation of mountain hydrology (Luce et al., 1998). Orographic enhancement of precipitation produces significantly greater quantities of precipitation in mountain ranges than

* Corresponding author. Fax: +1-605-394-5171.
E-mail address: tfontain@taz.sdsmt.edu (T.A. Fontaine).

0022-1694/02/$ - see front matter
PII: S0022-1694(02)00029-X

on the adjacent basins and plains (Barros and Lettenmaier, 1993; Hartman et al., 1999). In addition, a large percentage of precipitation falls as snow because mean temperatures decrease with elevation. Large volumes of water are stored in snowpack and subsequently released during spring and summer snowmelt. This cycle of water storage and release can be critical for agricultural economies, urban water supplies, groundwater recharge, hydropower, wildlife habitat, recreation, and navigation.

The importance of snowmelt in mountainous terrain has led to significant research in snowmelt modeling. Many models that deal strictly with snow accumulation and snowmelt have been developed (Martinec, 1960; Anderson, 1968, 1976; Rango and Martinec, 1979; Blöschl et al., 1991; Jordan, 1991; Garen and Marks, 1996; Coughlan and Running, 1997). Models range from complex energy balance models to more simplistic degree day based models. Rango and Martinec (1994) compared seven snowmelt runoff models and found that some of the models performed to a high degree of accuracy. However, these models are snowmelt models and do not model the entire surface and sub-surface water balance.

Models that deal extensively with snow accumulation and snowmelt in the simulation of total water budgets include the precipitation-runoff modeling system (PRMS), regional hydro-ecologic simulation system (RHESSys), and variable infiltration capacity (VIC) model. The United States Geological Survey (USGS) PRMS is a model designed to evaluate impacts of various combinations of precipitation, climate, and land use on streamflow, sediment yields, and general basin hydrology (Leavesley et al., 1983). RHESSys computes water and carbon budgets of terrestrial ecosystems (Band et al., 1993). The VIC model (Wood et al., 1992) simulates macroscale spatial variability of infiltration and runoff production as a spatial probability distribution. VIC has been used for long-term water supply and flood forecasting.

Although models exist that include snow processes with simulation of water balances, options are limited for application of these models in large river basins with limited data. Examples of these applications include water resources management, agricultural management, and evaluating impacts of potential climate change on water resources. An existing model that is capable of these types of analyses is the soil water assessment tool (SWAT). SWAT was initially developed for comprehensive modeling of the impacts of management practices on water yield, sediment yield, crop growth, and agricultural chemical yields in large ungaged basins (Arnold et al., 1998). SWAT is one of the few models that are designed to simulate water resource and agricultural issues at scales up to continental size without excessive data and calibration requirements.

During applications of SWAT for evaluating impacts of potential climate change on the water resources of the Missouri River Basin, it became apparent that the uncertainty associated with the hydrologic simulations in high altitude subbasins needed to be explored (Fontaine et al., 1999; Hotchkiss et al., 2000). Inadequate performance of the model in mountain basins was also reported by Arnold et al. (1999). Therefore, experiments were conducted to determine if SWAT could accurately simulate snow processes in large, mountainous basins. Existing algorithms were revised, and new algorithms added, to improve simulations in these conditions. This paper describes the results of these experiments and the revisions to the SWAT model.

2. Hydrologic model

Hydrologic modeling requires extensive amounts of information that include climate, soil type, land use, land cover, elevation, and geologic data. It is difficult to efficiently obtain and use this data when modeling large, remote, heterogeneous areas such as mountain basins. For large scale modeling to be a viable water resource management tool in alpine terrain, the model should be designed to run with relatively low data requirements and calibration effort, and to efficiently compute long-term simulations on a continuous basis.

The Agriculture Research Service of the United States Department of Agriculture developed SWAT to meet these requirements for successful large-scale modeling of mountain basins. SWAT is a continuous time model that operates on a daily time step. Model design objectives were to predict the long-term impact of management decisions on water, sediment, and agricultural chemical yields in large ungaged basins

with little to no calibration effort (Arnold et al., 1998). Due to the intensive data collection and data file creation efforts involved with large scale modeling, SWAT is designed to use the graphical resources analysis support system (GRASS) geographic information system (GIS) for the extraction of parameter values and model input data from various map layers and databases for large scale modeling. Data extracted and written to model input files include topographic, land use, soils, weather, and management information.

SWAT has been described in detail in many other references, including Arnold and Allen (1996) and Arnold et al. (1998), and therefore only a brief summary is given here. Model components include hydrology, weather, sedimentation, soil temperature, crop growth, nutrients, pesticides, and agricultural management. The computation of hydrologic processes operates in five phases: (1) precipitation interception, (2) surface runoff, (3) soil and root zone infiltration, (4) evapotranspiration and soil and snow evaporation, and (5) groundwater flow. A water balance equation calculates the change in soil water content (ΔSW) as:

$$\Delta SW = (P - Q - ET - DP - QR) \quad (1)$$

where P is the precipitation, Q the runoff, ET the evapotranspiration, DP the percolation, and QR the return flow.

Surface runoff volume is estimated by an enhanced Soil Conservation Service (SCS) curve number method. Average curve number values are derived from the relationships between soils, land use, management, and runoff. The curve number in SWAT is adjusted at each time step based on changes in soil water content. Soil and root zone infiltration are regulated as a function of soil water content and field capacity of the soil layer.

The SCS curve number relationships have resulted from over 20 years of intensive studies involving rainfall runoff relationships from rural watersheds. The method was developed to provide a consistent basis for estimating the amounts of runoff under varying land use and soil types. Loague and Freeze (1985) have shown that in many cases, simpler and less data-intensive methods such as curve number based models may provide as good or better simulations than more physically based models such as the Green–Ampt model. Physically based models require temporally and spatially disaggregated precipitation data, and more detailed soil information, which are not feasible to obtain or use in remote or large basins. In addition, many applications of physically based models end up using parameter values estimated from empirical relationships (King et al., 1999).

Plant, soil, and snow evaporation are computed separately as functions of potential evapotranspiration (ET). Plant transpiration is a function of available soil moisture, leaf area index, and potential ET. The data needed to calculate potential ET with the Penman–Monteith method are obtained by SWAT from a database containing meteorological statistics for the nearest National Oceanic and Atmospheric Administration (NOAA) observation station.

Groundwater movement in the shallow aquifer is represented by three processes: upward migration (and subsequent ET), seepage to a deep aquifer, and groundwater flow to a stream. Water percolating to the deep aquifer is lost from the system. Both upward migration and groundwater seepage to the deep aquifer are controlled by shallow aquifer storage, and by coefficients that regulate the rate of water loss. Lateral groundwater flow is based on a kinematic storage model and can recharge streamflow based on a groundwater recession parameter that lags and regulates the rate at which water is returned to the stream.

The original SWAT snowmelt component is similar to the simple degree day method used in the CREAMS model (Knisel, 1980). The rate of snow melt (mm/day) is estimated as 4.57 (maximum daily air temperature) on days when the maximum daily air temperature exceeds 0 °C. Meltwater is treated the same as rainfall for estimating runoff and percolation.

3. Study area

Several large mountainous watersheds throughout Wyoming and Montana, draining into the Missouri River Basin, were considered for this study. The Wind River Basin was ultimately selected because existing glaciological and snowmelt runoff research provided informative background data. The Upper Wind River Basin is located in west central Wyoming and is characterized by cold moist alpine regions, dry rugged mountains, and a dry flat basin floor (Fig. 1).

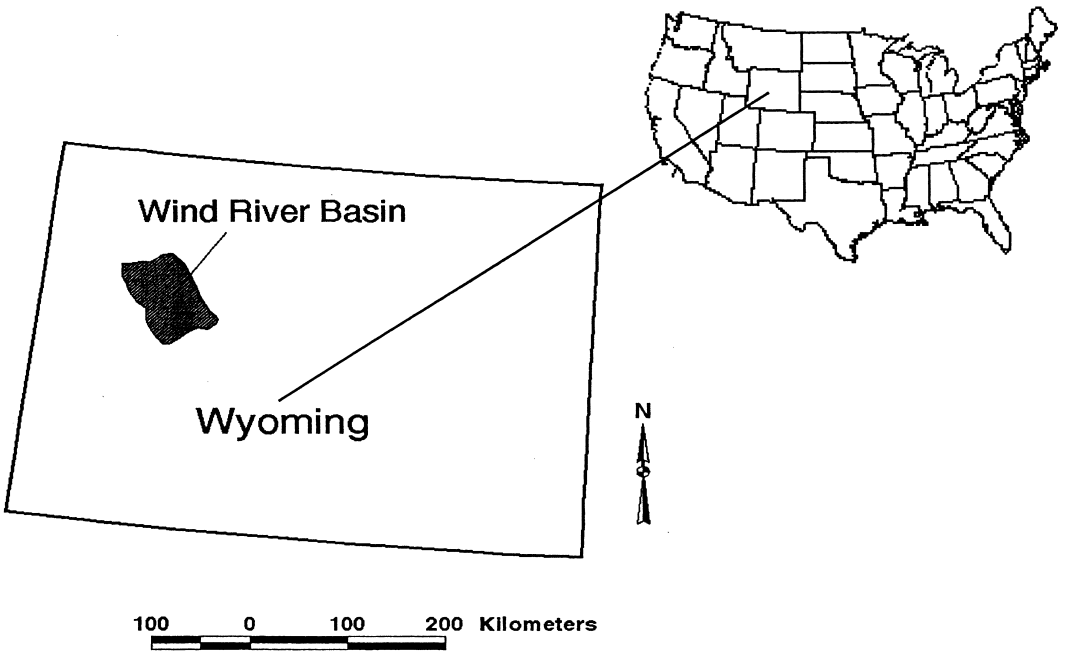

Fig. 1. Location of the Upper Wind River Basin in Wyoming.

The 4999 km^2 basin is surrounded on three sides by four mountain ranges: the Wind River Range, Gros Ventre Range, Absaroka Range, and the Owl Creek Range. Basin relief is extreme, ranging from the highest point in Wyoming at 4207 to 1865 m at the basin outlet, resulting in 2342 m of total relief within 50 km (Fig. 2). The basin is typical of the mountainous terrain of the Missouri River headwaters region and

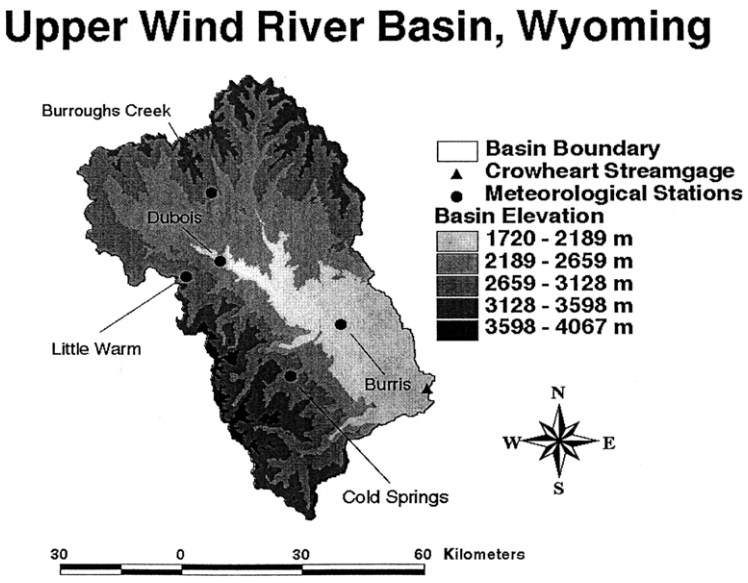

Fig. 2. Digital elevation model of the Upper Wind River Basin.

provides an excellent test case for evaluating and improving the SWAT model.

The climate of the basin is heavily influenced by topography. The Wind River, Gros Ventre, and Absaroka ranges are major impediments to synoptic-scale weather systems passing from the west and northwest to the Wind River Basin. As a result, there exists an extreme annual vertical precipitation gradient within the basin. The greatest precipitation amounts (up to 1250 mm/year) are found in the northwest portion of the basin where the Wind River, Gros Ventre, and Absaroka mountain ranges meet. Dubois, WY (1865 m), located approximately 30 km east of the continental divide in the narrow valley between the Wind River and Absaroka ranges, averages only 180 mm of precipitation per year.

The majority of precipitation falls as snow in the mountains surrounding the basin. Significant snowpack development begins in October. It is not until late March–May that the snowpack begins to progressively ripen and release melt water to the surface and near surface hydrologic system. The snowmelt is complicated by the elevation control on temperature and precipitation, allowing for significant temporal variability throughout the basin. As a result, the observed monthly streamflow of the Wind River displays pronounced seasonal cycles dominated by a spring and summer snowmelt peak followed by mid-winter baseflow.

Soil development and vegetative growth within the basin vary greatly. The crest of the range above tree line is primarily composed of exposed granitic bedrock and some shallow soil development supporting alpine tundra type vegetation. Permeability is dependent on bedrock fracturing beneath shallow soils. Glaciated and pre-glaciated cirques are filled with freshly exposed glacial till composed primarily of a matrix of granite clasts, sand, and rock flour. Within the valleys below tree line, glacial till coverage expands and vegetation and soil development increases. Permeability on most moderately glaciated tills is moderate to low. Vegetation and soil development on valley sides is dependent on slope with little to no development on the steeper walls. The basin floor is dry and sandy with freely draining soils, and the land cover is primarily rangeland with sagebrush and some areas of tall grasses.

4. Model setup

The graphical resource analysis support system (GRASS) geographic information system (GIS) was used to disaggregate the Upper Wind River Basin into smaller subbasins to reduce spatial heterogeneity (Fig. 2). The five subbasins ranged from 15 to 1645 km^2.

Model input data can be extracted from a variety of internal data bases and map coverages using the GRASS GIS interface. Data provided and extracted by this interface include: (1) land use data obtained through the 1 km resolution Land Use and Land Cover Digital Data (USGS_LUDA); (2) soil type and properties from the 1 km resolution State Soils Geographic Database (STATSGO) association map; and (3) topographic attributes from a 90 m resolution USGS digital elevation model (DEM). From these databases, and associated tables which describe typical ranges of physical parameters in SWAT, model input files with parameter values were created.

Within the SWAT/GRASS database for NOAA meteorological stations, the only meteorological stations within the basin boundaries are located on the basin floor and are not representative of the basin as a whole. To compensate for this problem, data from Snow Telemetry (SNOTEL) meteorological stations used by the US Department of Agriculture for the monitoring of snowpack conditions in mountainous terrain were obtained through the Centralized Forecast System database. All SNOTEL stations within and near the basin boundaries were entered into a GRASS database for use in the data extraction process. For each subbasin, SWAT selects one meteorological station closest to the centroid of each subbasin. Four meteorological stations were used: Cold Springs (2936 m) (SNOTEL), Little Warm (2933 m) (SNOTEL), Burroughs Creek (2668 m) (SNOTEL), and Burris (1864 m) (NOAA) (Fig. 2). Meteorological stations provided daily maximum and minimum temperature and daily liquid precipitation. Meteorological statistics required for computation of hydrometeorological processes such as ET, pond evaporation, and vegetation growth were obtained through the SWAT/GRASS NOAA meteorological station database. Statistics extracted from the Dubois, WY station include solar radiation, 10 year frequency for half hour and 6 h water equivalent precipitation, monthly maximum half-hour water

equivalent precipitation, average monthly temperature statistics, humidity, wind speed, and number of precipitation days per month.

5. Selection of parameters and initial simulation

Part of the original motivation for the coupling of SWAT and the GRASS GIS was to create a hydrologic model that could be used in large river basins with little to no calibration (Arnold and Allen, 1996). Minimized calibration requirements allow model applications in large basins where extensive input parameter selection and calibration efforts are either impossible because of inadequate data, or are too uncertain or time consuming for project objectives. While this approach is obviously inappropriate for many models and modeling applications, there are cases where simulations with little to no calibration are useful. Model results must simply be interpreted in light of this approach.

SWAT is not a parametric model requiring a formal calibration procedure to optimize parameter values using simulated vs. observed results. Instead, the model was designed so that the GRASS interface can characterize basin processes using readily available GIS databases and meteorological information, combined with internal model libraries. Parameters have physical meanings in the field, allowing parameters to be set using these databases for land use and cover, soil type, topography, and climate statistics. Several studies have demonstrated that the GRASS GIS interface can successfully select input parameter values for SWAT without calibration in a wide variety of hydrologic systems and geographic locations using the readily available GIS databases (Manguerra and Engle, 1998; Srinivasan et al., 1998; Arnold et al., 1999; King et al., 1999). In cases where additional model accuracy is needed, subsequent minor adjustment of a few parameters may improve simulated output by accounting for site-specific conditions. However, this fine-tuning is optional, and is only possible where reliable data are available.

Our model application to evaluate the potential accuracy of SWAT for simulating snow processes in remote mountain basins followed the conventional approach described earlier for allowing the model and GRASS interface to select parameter values without formal calibration. A 6 year (1991–1996) hydrologic simulation was conducted following a 7 year model warm up period that used data from 1990 to 1996. The warm up period established appropriate initial conditions for groundwater and soil water storage. Initial input parameters for the Upper Wind River Basin were automatically extracted from the GRASS GIS databases. Minor refinements to the extracted data were made because the databases and map coverages lack detail and have coarse spatial resolution for this region. Refinements were based on tables in the SWAT manual containing ranges of typical values derived for soil and land cover types from existing databases and prior research (Sammons et al., 1995). Additional information was also obtained from two field reconnaissance trips, soil surveys from the Natural Resources Conservation Service, irrigation information from the Wind River Bureau of Indian Affairs, and related climate and snow data available from NOAA, and from the USGS in Salt Lake City, Utah (Naftz and Smith, 1993). A very limited amount of additional parameter adjustment was used to determine if simulated discharge could be improved. Values related to channel dimensions, curve numbers, soil properties, land use, and groundwater constants were changed, one at a time, to influence the timing and peak discharge values of the seasonal hydrograph. Impacts on simulated discharge were relatively minor, and were related to changed curve numbers and parameters for groundwater recession, which is consistent with other SWAT research (Srinivasan et al., 1998).

Simulation results were compared to the observed monthly Wind River streamflow. The primary modeling objectives involve snowmelt processes, and therefore emphasis was placed on initiation of snowmelt, peak streamflow, time of peak streamflow, and the recession limb. Three prominent features exist in the seasonal flow patterns: (1) a rapid increase in streamflow beginning in late April, (2) peak streamflow during late June to July followed by a slow recession of discharge, and (3) late October–early March discharge composed entirely of baseflow.

Results from the initial 6 year simulation demonstrated a poor correlation to the observed streamflow, with an average annual Nash–Sutcliffe R^2 of -0.70 (Nash and Sutcliffe, 1970). The difference between

Table 1
Input parameters used for final simulation

Input parameter	Value
Elevation bands	1720–2189 m
	2189–2659 m
	2659–3128 m
	3128–3598 m
	3598–4067 m
Precipitation lapse rate (dP/dZ)	0.5 mm/km
Temperature lapse rate (dT/dZ)	− 5.0 °C/km
Rain/snow threshold (T_s)	1.0 °C
Maximum melt coefficient (α_{mx})	6.5 mm/°C
Minimum melt coefficient (α_{mn})	4.0 mm/°C
Snowpack temperature lag factor (β)	0.5
Snowpack temperature melt threshold (T_m)	0.0 °C
Areal snow coverage threshold: cov_{100}	300.0 mm
Areal snow coverage threshold: cov_{50}	0.5

the total observed and simulated streamflow (D_v) was 22.5%. Five major problems were identified with the simulated hydrograph in Fig. 4. The rising hydrograph limb began too early. Peak discharges were, in general, smaller than observed discharges. Several discharge sub-peaks were simulated instead of one primary peak discharge. The recession limb of the hydrograph began too early. Streamflow for approximately 4 months of each year approached 0.0 m^3/s.

Much of the simulated hydrograph error was attributed to the poor treatment of the snowmelt process. SWAT was unable to represent the spatial and temporal variability of climate within the basin. The premature increase in streamflow suggested that simulated snowmelt was occurring too early throughout the basin. Erroneous peak streamflow was the result of several factors: (1) improper handling of the elevation controlled temporal variability in the snowmelt process; (2) poor simulation of volumetric meltwater production; and (3) unrepresentative precipitation data. Recession limb errors were related to poor modeling of the temporal variability of late season snowmelt contributions from the highest basin elevations to baseflow. Model algorithm improvements were needed to better simulate the seasonal progression of snowpack evolution and meltwater production throughout the climate-elevation zones.

6. Snowmelt algorithms

To improve the simulation of the hydrologic and atmospheric processes that govern snowmelt in mountainous terrain, algorithms were modified or added to the model. The algorithms were developed to be consistent with the original objectives for SWAT, by permitting efficient, continuous simulation in large ungaged basins where available data are limited or potentially unrepresentative, and by providing reasonably accurate simulation results without calibration. The following discussion describes algorithm additions and improvements, physical reasoning behind algorithms, and user guidelines for the operation of the snowmelt routine.

6.1. Elevation bands

Most snowmelt runoff models handle spatial and temporal variations due to elevation by incorporating elevation bands or zones allowing the model to discretize the snowmelt process based on basin topographic controls (Rango and Martinec, 1979, 1994; Hartman et al., 1999). The ability to represent up to 10 elevation bands within each subbasin was added to SWAT. Within the subbasin input files, the average elevation of each elevation band is entered, followed by the percentage of the subbasin area within that band. Five elevation bands were established for four of the five subbasins in the Upper Wind River Basin (Table 1). The fifth subbasin has a small elevation range and therefore only one elevation band was required.

6.2. Temperature lapse rate

To accurately represent temperature throughout an elevationally diverse subbasin, a temperature lapse rate is applied to each elevation band (Rango and Martinec, 1979, 1994; Martinec and Rango, 1986; Garen and Marks, 1996; Hartman et al., 1999). Atmospheric temperatures within the troposphere generally decrease with elevation. To compute a local lapse rate for the Wind River Basin, 10 SNOTEL, one NOAA, and one independent observing station within and close to the Upper Wind River Basin were used to develop a relationship between mean annual temperature and station elevation. SNOTEL stations typically did not have temperature information until after 1989.

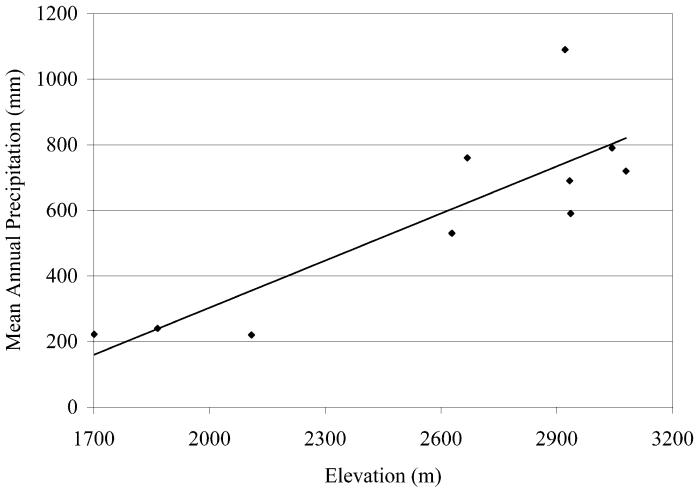

Fig. 3. Wind River Basin mean annual precipitation vs. elevation.

Therefore, 1990–1996 mean annual temperatures were used to calculate the lapse rate. The independent observing station was installed at 3963 m beside the Fremont Glacier in the Wind River Range by Naftz and Smith (1993) during the period 11 July, 1990–10 July, 1991 for glaciological investigations.

A mean local basin lapse rate (dT/dZ) of -5 °C/1000 m was calculated for use in all subbasins, based on data from the 12 observation stations. Subbasin temperatures are adjusted within each elevation band by comparing the elevation band midpoint elevation (Z_B) with the station elevation (Z). The elevation difference is multiplied by the lapse rate to calculate a temperature difference between the station elevation and the elevation band. An updated elevation band mean temperature (T_B) is calculated by adding or subtracting the temperature difference to the temperature measured at the station elevation (T).

$$T_B = T + (Z_B - Z)dT/dZ \quad (2)$$

6.3. Precipitation lapse rate

The model selects only one meteorological station for each subbasin. Therefore, spatially heterogeneous precipitation regimes may be poorly represented within a subbasin. Four meteorological stations were assigned by the model to the five-basin representation of the Upper Wind River Basin. The four meteorological stations were unrepresentative of the precipitation within the basin as a whole because the basin is large and precipitation regimes within the basin are varied. An algorithm was developed to better represent the actual distribution of precipitation with elevation.

The increase in precipitation with elevation has been well documented. The actual rate of precipitation increase with elevation can vary widely depending on the type of storm system and the direction of travel (Peck, 1972). However, middle latitude (including Wyoming) precipitation typically increases continually with elevation (Barry, 1992a). In the Colorado Rocky Mountains, precipitation at 3200 m is nearly six times the precipitation that occurs at the base of the western slopes at 1750 m (Hjermstad, 1970). Hanson (1982) showed a strong linear relationship of increasing precipitation with elevation on both windward and lee slopes in southwest Idaho. Hanson also found that the strongest precipitation–elevation relationship occurred during winter when advective influences were greatest, whereas the convectively enhanced precipitation in summer showed a weak relationship to elevation.

To accommodate mesoscale and synoptic scale orographic influences, a precipitation-lapse rate has been added to the snowfall routine. The routine is similar to that described by Running et al. (1987), Blöschl et al. (1991) and Hartman et al. (1999). The precipitation adjustment according to elevation has been added only to the snowfall routine. Summertime adjustment is less critical because 7 to 8 months of the

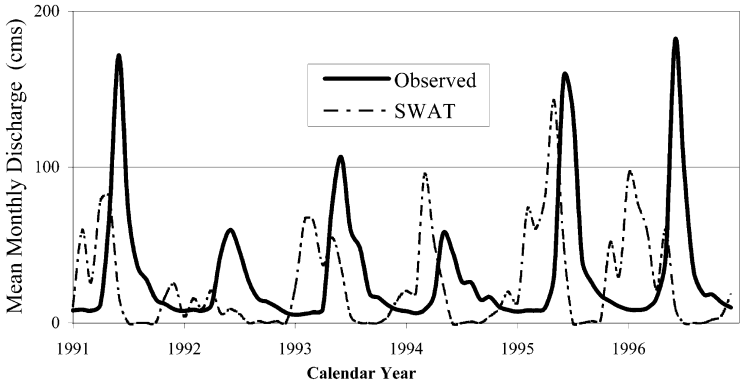

Fig. 4. Final Upper Wind River SWAT simulated monthly streamflow prior to model modification.

year are dominated by snowfall, and according to Hanson, summertime convective precipitation is weakly related to elevation.

A lapse rate for annual precipitation was found by plotting mean annual precipitation vs. station elevation. Precipitation data from a total of 10 SNOTEL and NOAA meteorological stations located within and near the Upper Wind River Basin were plotted against station elevation (Fig. 3). The slope of the elevation vs. precipitation plot demonstrated that annual precipitation increased with elevation at the rate of +0.5 mm/m.

SWAT operates on a daily time step and defines precipitation events as the volume of precipitation that falls in a 24 h period. Therefore, an event scale precipitation lapse rate was derived for use at a daily time step. The event scale lapse rate was computed by distributing the mean annual precipitation lapse rate (+0.5 mm/m) among all of the precipitation events that occurred during 1 year. The model uses one precipitation lapse rate value for all subbasins.

The precipitation lapse rate (dP/dZ) value for the daily time step used in this analysis was +0.5 mm/km per event. Adjusted precipitation in each elevation band (P_B) is based on the difference between the elevations of the subbasin meteorological station (Z) and each elevation band (Z_B), multiplied by the lapse rate of +0.5 mm/km per event.

$$P_B = P + (Z_B - Z)dP/dZ \quad (3)$$

6.4. Rain/snow threshold

The determination of whether the precipitation is rain or snow is made by considering the daily mean temperature within a subbasin. If the elevation corrected mean daily temperature (T_B) within a subbasin elevation band is below a critical temperature (T_S), then the precipitation within that elevation band is snow. Numerous studies have shown that a threshold temperature can be used to determine the type of precipitation on a statistical basis. In the Himalayas, the rain/snow threshold increases from near 1 °C at 500 m to 4 °C at 3500–4000 m Barry (1992b). Many snowmelt runoff models use a critical temperature for the determination of precipitation type (Anderson, 1973; Martinec and Rango, 1986). This analysis uses 1 °C for T_S.

6.5. Snowpack accumulation

Snowpack is represented as snow water equivalent (SWE). During a time step, snowpack can be increased by the water equivalent of snowfall (P_{SB}), decreased by the release of meltwater (M), or decreased by sublimation (E_S):

$$SWE_2 = SWE_1 + P_{SB} - M - E_S \quad (4)$$

Rain is not added to snowpack since P_{SB} is only nonzero in Eq. (4) when $T_B < T_S$. Rain falling on snow covered ground is treated the same as rain on bare ground. When the criteria for release of meltwater are satisfied, released meltwater is treated as rainfall. Sublimation (E_S) from the snow surface is computed as a function of potential evapotranspiration (ET).

The meltwater released (M) in Eq. (4) will be zero until snowpack temperature exceeds a minimum

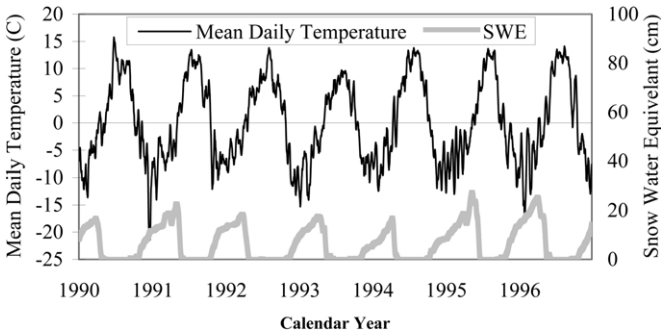

Fig. 5. Ten-day running mean of daily temperature and daily SWE for Cold Springs SNOTEL station (elevation 2936 m).

threshold temperature. Once this temperature is exceeded, M is calculated based on temperature conditions, a variable melt rate, and on the amount of snowcover present in the catchment. These calculations are described in the following sections for snowpack temperature, potential snowmelt, and areal snow coverage.

6.6. Snowpack temperature

A snowpack cannot begin to melt and release water before the entire pack has reached 0 °C. A routine has been added which prevents snowmelt release when the snowpack temperature (T_{SN}) is below a threshold (T_m), which is typically set to 0 °C. Snowpack temperature can be influenced by many local variables, including air temperature, snowpack density, snowpack depth, and exposure. The revised snow component assumes that snowpack temperature at depth below the snow surface can be estimated as a function of the mean daily temperature during the preceding days (Anderson, 1973). The updated snowpack temperature (T_{SN2}) is lagged based on a coefficient (β) that relates daily mean air temperature (T_B) to snowpack temperature (T_{SN1}).

$$T_{SN2} = T_{SN1}(1.0 - \beta) + T_B\beta \quad (5)$$

The snowpack temperature lag factor (β) is a constant with permissible values ranging from 0 (low reliance on air temperature during previous days) to 1 (snowpack temperature is equal to mean daily air temperature). The selection of an appropriate value for β will primarily depend on the depth of snowpack. Values for β in areas typified by deep snowpack will be in the approximate range of 0.0–0.5. Areas typified by shallow snowpack will have β values in the approximate range of 0.5–1.0.The temperature at which the snowpack begins to melt (T_m) is adjustable.

6.7. Potential snowmelt calculation

To accurately model the rate and volume of meltwater released (M) during melting, a relationship between the snowpack energy budget and melt rate must be developed. In mountainous areas, the relationship must often be determined using temperature because complete meteorological data for calculating an energy budget such as humidity, radiation, and wind speed are generally not available. Fortunately, the temperature–melt rate relationship is strong in the majority of situations (Martinec, 1960; Martinec and Rango, 1981; Rango and Martinec, 1995; Cline, 1997). A melt coefficient (α) relates degrees above a melt threshold T_m to the amount of meltwater released (M).

Measures of temperature considered for modeling snowmelt included daily mean air temperature, maximum daily air temperature, and a combination of daily mean air and snowpack temperatures. A strong correlation existed between maximum SWE and the point at which mean air temperatures reach 0 °C (Fig. 5). The SWE began to drop sharply, indicating the start of the snowmelt period, near the date when mean daily air temperature initially equaled 0 °C. In contrast, little correlation was observed between maximum SWE and maximum temperatures at or above 0 °C. Therefore, the snowpack temperature (T_{SN}) and mean daily temperatures were used along with a melt coefficient (α) to calculate potential volume of meltwater as:

$$M = \alpha(((T_{SN} + T_B)/2) - T_m) \quad (6)$$

The melt rate from a snowpack is not a fixed value; rather it changes in response to snowpack conditions (Martinec and Rango, 1986). The ability of a snowpack to release meltwater is dependent on the snowpack temperature and free water content. All energy gained by a snowpack must first be used to bring the snowpack temperature to 0 °C. Once the snowpack is isothermal, additional energy begins to melt snow and increase the free water content of the snowpack. The eventual saturation of a snowpack by free water initiates meltwater release.

The most important variables affecting the melt rate are the water content, snow surface albedo, and intensity of short wave solar radiation. Snowpack densities range widely but will typically fall between 0.20 and 0.60 g/cm^3. Snow surface albedo decreases during the melt season in response to water saturation and increasing dust concentrations and surface detritus (Warren and Wiscombe, 1980; Conway et al., 1996). The intensity of short-wave solar radiation incident and reflected on a snowpack increases as the summer solstice approaches, resulting in warmer ambient air temperatures and an increase in snow surface melt.

Solar radiation intensity is a dominant factor in the determination of the melt coefficient in the mid-latitudes. Results from the Central Sierra Snow Laboratory (Anderson, 1968, 1973) show that the seasonal variation in the melt coefficient can be approximated by a sine function. This approach defines a minimum (α_{mn}) and maximum (α_{mx}) melt factor assumed to occur on 21 December and 21 June, respectively. Therefore, a sinusoidal varying melt coefficient is used to represent the natural snowpack saturation process. The appropriate melt coefficients will approximately range between 0.20 and 0.60 cm/deg. (Martinec, 1960; Martinec and Rango, 1986; Rango and Martinec, 1995). The meltwater coefficient used in Eq. (6) is therefore calculated as:

$$\alpha = (\alpha_{mx} + \alpha_{mn})/2 + (\sin[(\text{day of year})\pi/366])(\alpha_{mx} - \alpha_{mn})/2 \quad (7)$$

6.8. Adjustment for areal snow coverage

The actual volume of meltwater released during a melt event depends on the potential melt volume (Eq. (6)) and the extent of snow coverage (Shook and Gray, 1997). During the melt season, there exists a snowline which moves upward in elevation as melting progresses. The decrease in available snow water during a melt season must be taken into account to accurately estimate the actual melt volume. The rate of snow cover depletion has been shown to be a function of how much bare ground remains covered by snow (Anderson, 1968). Factors that are similar from year to year, such as aspect, vegetation, and weather patterns, define a snow cover areal depletion curve that is unique to each area (Blöschl et al., 1991; Elder et al., 1991; Hartman et al., 1999).

A method using an areal depletion curve has been adopted from Anderson (1973). This method compensates for reduced areal snow coverage by adjusting potential meltwater values that are based on 100% areal snow coverage. An areal depletion curve is a plot of the areal extent of snow cover vs. a ratio describing how much of the original snow water remains. For example, for a subbasin to have 100% snow coverage, the total SWE must remain above a threshold SWE value. If the subbasin SWE falls below the 100% snow coverage threshold, then a snowcover less than 100% is assumed. Snow coverage less than 100% reduces the available melt volume. The actual SWE threshold values will be unique to each subbasin and will depend on factors such as vegetation distribution, wind loading of snow, wind scouring of snow, interception, and aspect.

The adopted routine adjusts the potential meltwater (M) calculated in Eq. (6) to an actual volume of meltwater (M_A) released, based on the areal extent of snow cover. The method uses an areal depletion curve estimated as a logarithm. The curve ordinate is defined by

$$yy = \text{SWE}/\text{cov}_{100} \quad (8)$$

where yy is the fraction of snow water equivalent relative to 100% snow coverage, SWE is the current SWE in an elevation band, and cov_{100} is the SWE threshold at which 100% snow cover exists. The curve abscissa (cov) is the areal extent of snow cover expressed as a fraction.

The shape of the depletion curve is fixed before snowmelt simulation begins. The curve shape is defined by three points that are fixed at (0.0,0.0), (0.95,0.95), and (0.5,cov_{50}). The curve shape is adjusted using the input parameter cov_{50}, which is a

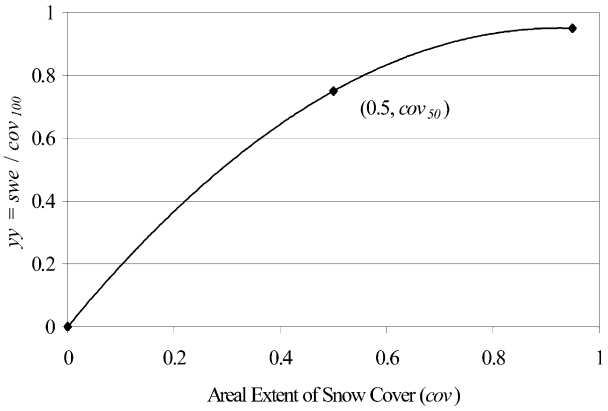

Fig. 6. Areal depletion curve.

fraction defined as the ratio of SWE at 50% areal snow cover and SWE at 100% snow cover. Varying cov_{50} between 0 and 1 allows the user to change the shape of the curve and represent different areal depletion curves depending on the area of interest. An area typified by wide ranging snow cover depths (such that areas devoid of snow cover exist) dictates a value of cov_{50} that approaches 1.0. Conversely, an area typified by uniform snow cover depths (such that at all times there exists a uniform snow cover) dictates a value of cov_{50} that approaches 0.0. An example of a user defined areal depletion curve is shown in Fig. 6 with the user defined coordinate (cov_{50}) set to 0.75.

To determine the decrease in available melt water at each simulation time step, Eq. (8) is solved for *yy*. This value of *yy* is used to calculate the areal extent of snow cover (cov) as

$$\mathrm{cov} = yy/(yy + \exp(\mathrm{cov}_1 - \mathrm{cov}_2(yy))) \quad (9)$$

where cov_1 and cov_2 are internally calculated points that define the shape of the depletion curve. The product of the areal extent of snow cover fraction from Eq. (9) and the potential meltwater value (M) from Eq. (6) determines the actual volume of meltwater (M_A) released

$$M_A = M\,\mathrm{cov} \quad (10)$$

If the SWE within an elevation band drops below the SWE threshold for 100% areal coverage, then the area within the elevation band is not fully covered by snow and the potential meltwater available for release is reduced. Once the 100% areal coverage depth is exceeded, the area within the elevation band is completely covered with snow and the total volume of potential meltwater is available for release. This method inherently compensates for melt variations due to exposure, wind loading, and scouring of snow.

7. Snow parameter selection

The snow algorithms were developed to allow application with relatively little to no calibration data and effort. Some values, such as T_S, T_m, α_{mx}, and α_{mn}, were simply set based on information from the literature. Data from remote mountain meteorological stations were used in this study to set some of the other parameters in the snowmelt algorithms, including temperature and precipitation lapse rates, β, cov_{50}, and cov_{100}. These parameters could be estimated for basins without higher elevation meteorological stations. Minor adjustment of some of the parameters was used to account for differences between the micro scale climate at each meteorological station, and the relatively large, heterogeneous areas within elevation bands and subbasins. Table 1 contains the input parameter values used in the snowmelt routines for the final Upper Wind River hydrograph simulation.

8. Final simulation and results

The 6 year hydrologic simulation of the Upper Wind River Basin was repeated using the newly

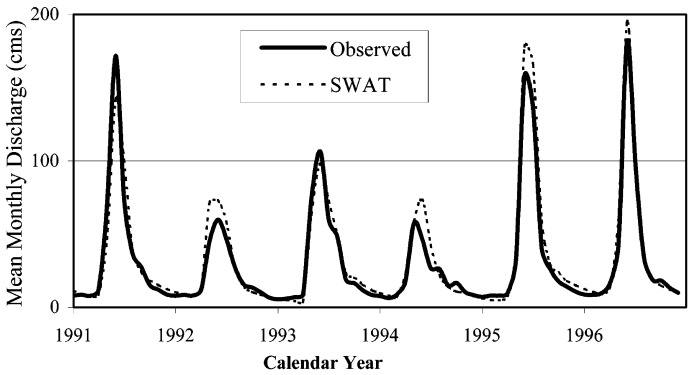

Fig. 7. Final Upper Wind River SWAT simulated monthly streamflow after model modification.

adopted snowmelt algorithms. All original input parameters remained identical to the initial simulation with the exception of groundwater parameters. The groundwater parameters were adjusted because of the significant change in groundwater recharge related to the addition of the new snowmelt algorithms. Simulated and observed monthly streamflow for the 6 year period compared very well (Fig. 7). The average annual Nash–Sutcliffe R^2 efficiency between the simulated and the observed streamflow was $+0.86$. The percentage difference between the total observed and simulated streamflow (D_v) was -9.8%.

The five major problems identified in the initial simulation were significantly improved. Initiation of snowmelt and timing of peak streamflow were clearly improved. Peak streamflow in 3 of 6 years was several m^3/s greater than the observed, however, percent errors were small. Timing of the recession limbs was accurate. Dry season baseflow simulation was correct to within 1–3 m^3/s in each year.

9. Conclusions

Although the SWAT hydrologic model was designed with the capability of simulating up to continental scale basins, it was primarily intended for agricultural regions and not for heterogeneous mountain basins. Initial Upper Wind River modeling results indicated limitations in the ability of the model to handle large, snowmelt dominated, mountain basins. The hydrologic and atmospheric processes governing snowfall and snowmelt for this basin were identified. With the governing processes identified and parameterized, hydrologic simulation of the Upper Wind River was significantly improved.

Modeling success was attained by identifying climatic variables that were poorly resolved by the initial snowmelt routine. The most important issue identified was the role of elevation in the spatial and temporal evolution of the state of snowpack. Algorithm adjustments were made to simulate the increased volume of precipitation events observed in areas of moderate to high elevation. Variation in air and snow temperatures with elevation was represented in the new model algorithms. The incorporation of an adjustable meltwater production factor to accommodate a seasonally evolving snowpack was successful. An algorithm was added to estimate the areal ground coverage of snow with respect to snow depth; this modification effectively simulates a dynamic snow line demarking the available snow water. The revised and new algorithms were designed to allow application to large basins with minimal to no calibration effort and data. The modeling success obtained in the Upper Wind River basin suggests that SWAT has the potential to be reliably applied to non-agricultural mountainous regions in the middle latitudes.

Acknowledgements

This research was supported in part by the Biological and Environmental Research Program (BER), U.S. Department of Energy, through the Great Plains

Regional Center of the National Institute for Global Environmental Change (NIGEC) under Cooperative Agreement No. DE-FC03-90ER61010. Additional support was provided by the South Dakota School of Mines and Technology. Appreciation is extended to Bill Capehart, Mark Hjelmfelt and Scott Kenner for manuscript review.

References

Anderson, E.A., 1968. Development and testing of snow pack energy balance equations. Water Resour. Res. 4 (1), 19–37.

Anderson, E.A., 1973. National Weather Service River Forecast System—Snow Accumulation and Ablation Model. , NOAA Technical Memorandum NWS Hydro, vol. 17. US Department of Commerce, Washington, DC p. 217.

Anderson, E.A., 1976. A point energy and mass balance model of snow cover. NOAA Technical Report NWS 19, US Department of Commerce, Silver Spring, Md., 150 pp.

Arnold, J.G., Allen, P.M., 1996. Simulating hydrologic budgets for three Illinois watersheds. J. Hydrol. 176, 55–77.

Arnold, J.G., Srinivasan, R., Muttiah, R.S., Williams, J.R., 1998. Large area hydrologic modeling and assessment—Part I: model development. J. Am. Water Resour. Assoc. 34 (1), 73–89.

Arnold, J.G., Srinivasan, R., Muttiah, R.S., Allen, P.M., 1999. Continental scale simulation of the hydrologic balance. J. Am. Water Resour. Assoc. 35 (5), 1037–1051.

Band, L.E., Patterson, R., Nemani, R., Running, S.W., 1993. Forest ecosystem processes at the watershed scale: incorporating hillslope hydrology. Agric. For. Meteorol. 63, 93–126.

Barros, A.P., Lettenmaier, D.P., 1993. Dynamics modeling of the spatial distribution of precipitation in remote mountainous areas. Monthly Weather Rev. 121, 1195–1214.

Barry, R.G., 1992a. Mountain Weather and Climate. 2nd ed. Routledge, New York pp. 226–259.

Barry, R.G., 1992b. Mountain Weather and Climate. 2nd ed. Routledge, New York pp. 239–243.

Blöschl, G., Kirnbauer, R., Gutknecht, D., 1991. Distributed snowmelt simulations in an alpine catchment, 1, model evaluation on the basis of snow cover pattern. Water Resour. Res. 27, 3171–3179.

Cline, D.W., 1997. Effect of seasonality of snow accumulation and melt on snow surface energy exchanges at a continental alpine site. J. Appl. Meteorol. 36, 32–51.

Conway, H., Gades, A., Raymond, C.F., 1996. Albedo of dirty snow conditions of melt. Water Resour. Res. 32 (6), 1713–1718.

Coughlan, J.C., Running, S.W., 1997. Regional ecosystem simulation: a general model for simulating snow accumulation and melt in mountainous terrain. Landsc. Ecol. 12, 119–136.

Davis, R.E., Marks, D., 1980. Undisturbed measurement of the energy and mass balance of deep alpine snow cover. Proceedings of the Western Snow Conference. vol. 48, pp. 62–67.

Elder, K., Dozier, J., Michaelsen, J., 1991. Snow accumulation and distribution in an alpine watershed. Water Resour. Res. 27 (7), 1541–1552.

Fontaine, T.A., Cruickshank, T.S., Stonefelt, M.D., Kenner, S.J., Hotchkiss, R.H., 1999. Hydrologic assessment of regional climate change impacts in large heterogeneous river basins. Potential consequences of climate variability and change to water resources of the US, Proceedings of the Atlanta Conference, American Water Resources Association, pp. 291–296.

Garen, D.C., Marks, D., 1996. Spatial distributed snow modelling in mountainous regions: Boise River application, HydroGIS 96: application of geographic information systems in hydrology and water resoources management. Proceedings of the Vienna Conference, April, 1996, IAHS Publication N. 235.

Hanson, C.L., 1982. Distribution and stochastic generation of annual and monthly precipitation on a mountainous watershed in southwest Idaho. Water Resour. Bull. 18, 875–883.

Hartman, M.D., Baron, J.S., Lammers, R.B., Cline, D.W., Band, L.E., Liston, G.E., Tague, C., 1999. Simulations of snow distribution and hydrology in a mountain basin. Water Resour. Res. 35 (5), 1587–1603.

Hjermstad, L.M., 1970. The Influence of Meteorological Parameters on the Distribution of Precipitation across Central Colorado Mountains. Atmospheric Science Paper, No. 163. Colorado State University, Fort Collins.

Hotchkiss, R.H., Jorgensen, S.F., Stone, M.C., Fontaine, T.A., 2000. Regulated river modeling for climate change impact assessment: the Missouri River. J. Am. Water Resour. Assoc. 36, 375–386.

Jordan, R., 1991. A one-dimensional temperature model for a snowcover. Special Report 91–16, US Army Cold Regions Research and Engineering Lab., Hanover, NH.

King, K.W., Arnold, J.G., Bingner, R.L., 1999. A comparison of two excess rainfall runoff modeling procedures on a large basin. Trans. ASCE, Am. Soc. Agric. Engr. 42 (4), 919–925.

Knisel, W.G., 1980. CREAMS, a field scale model for chemicals, runoff, and erosion from agricultural management systems, US Dept. Agric. Conserv. Res. Rept. No. 26.

Leavesley, G.H., Lichty, R.W., Troutman, B.M., Saindon, L.G., 1983. Precipitation–runoff modeling system: user's manual. US Geological Survey Water-Resources Investigations Report 83–4238, 207 p.

Loague, K.M., Freeze, R.A., 1985. A comparison of rainfall runoff modeling techniques on small upland catchments. Water Resour. Res. 21 (2), 229–248.

Luce, C.H., Tarboton, D.G., Cooley, K.R., 1998. Subgrid parameterization of snow distribution for an energy and mass balance snow cover model. International Conference on Snow Hydrology, October 1998, Brownsville, VT.

Manguerra, H.B., Engel, B.A., 1998. Hydrologic parameterization of watersheds for runoff prediction using SWAT. J. Am. Water Resour. Assoc. 34, 1149–1162.

Marks, D., Dozier, J., Davis, R.E., 1992. Climate and energy exchange at the snow surface in the alpine region of the Sierra Nevada. 1. Meteorological measurements and monitoring. Water Resour. Res. 28 (11), 3029–3042.

Martinec, J., 1960. The Degree-Day Factor for Snowmelt–Runoff Forecasting, vol. 51. IAHS-AISH Publications pp. 468–477.

Martinec, J., Rango, A., 1981. Areal distribution of snow cover

water equivalent evaluated by snow cover monitoring. Water Resour. Res. 17 (5), 1480–1488.

Martinec, J., Rango, A., 1986. Parameter values for snowmelt runoff models. J. Hydrol. 84, 197–219.

Naftz, D.L., Smith, M.E., 1993. Ice thickness, ablation, and other glaciological measurements on Upper Fremont Glacier, Wyoming. Phys. Geogr. 14, 404–414.

Nash, J.E., Sutcliffe, J.V., 1970. River flow forecasting through conceptual models. Part 1—a discussion of principles. J. Hydrol. 10 (3), 282–290.

Peck, E.L., 1972. Relation of orographic precipitation patterns to meteorological parameters. Distribution of precipitation in mountainous areas, vol. 11, Geneva, World Meteorological Organization, N. 326, pp. 234–242.

Rango, A., Martinec, J., 1979. Application of a snowmelt-runoff model using landsat data. Nord. Hydrol. 10, 228–235.

Rango, A., Martinec, J., 1994. Model accuracy in snowmelt runoff forecasts extending from 1 to 20 days. Water Resour. Bull. 30 (3), 463–470.

Rango, A., Martinec, J., 1995. Revisiting the degree-day method for snowmelt computations. Water Resour. Bull. 31 (4), 657–669.

Running, S., Nemani, R., Hungerford, R., 1987. Extrapolation of synoptic meteorological data in mountainous terrain and its use for simulating forest evapotranspiration and photosynthesis. Can. J. For. Res. 17, 472–483.

Sammons, N., Arnold, J., Srinivasan, R., Muttiah, R., Griggs, R., 1995. Users' Manual: Watershed Modeling and GIS with SWAT and GRASS. Blackland Research Center and Grassland, Soil and Water Research Laboratory, Temple, TX.

Shook, K., Gray, D.M., 1997. Synthesizing shallow seasonal snow cover. Water Resour. Res. 33 (3), 419–426.

Srinivasan, R., Ramanarayanan, T.S., Arnold, J.G., Bednarz, S.T., 1998. Large area hydrologic modelling and assessment. Part II: model application. J. Am. Water Resour. Assoc. 34 (1), 91–101.

Warren, S.G., Wiscombe, W.J., 1980. A model for the spectral albedo of snow, II, snow containing atmospheric aerosols. J. Atmos. Sci. 37, 2734–2745.

Wood, E.E., Lettenmaier, D.P., Zartarian, V.G., 1992. A land-surface hydrology parameterization with subgrid variability for general circulation model. JGR 97 (D3), 2717–2728.